

Study of Action Potential Propagation in Cardiac Tissues Using Cable Theory

NATELA ZIRAKASHVILI^{1*}, TEONA ZIRAKASHVILI^{2,3}

¹I. Vekua Institute of Applied Mathematics,
Iv. Javakhishvili Tbilisi State University,
11 University St., 0179, Tbilisi,
GEORGIA

²Ilia State University,
Tbilisi,
GEORGIA

³Tbilisi Heart and Vascular Clinic LTD,
Tbilisi,
GEORGIA

**Corresponding Author*

Abstract: - The goal of the present paper is to study the propagation of action potential in cardiac tissue using the cable equation. The paper discusses one-dimensional models of continuously coupled myocytes. Electrical behavior in cardiac tissue is averaged over many cells. Therefore, the transmembrane potential behavior for a single cell is studied. Using the monodomain model, in the absence of current at the beginning and end of the cable (cell), the initial boundary problem is posed and solved analytically. The paper also discusses a one-dimensional mathematical model of conduction in discretely coupled myocytes. The electrical behavior in the tissue is studied in individual myocytes, each of which is modeled as a continuum connected through conditions at the cell boundaries, which represent gap junctions. A stationary passive problem with Dirichlet boundary conditions is stated and solved analytically using the bidomain model. The problems are solved by the method of separation of variables. Numerical modeling of transmembrane potential propagation is performed using MATLAB software. Transmembrane isopotential contours, and 2D and 3D graphs corresponding to the obtained numerical results are presented.

Key-Words: - Cardiomyocytes; transmembrane potentials ; passive 1D cable equation; monodomain model; bidomain model

Received: July 12, 2022. Revised: September 28, 2023. Accepted: October 8, 2023. Published: October 16, 2023.

1 Introduction

The article studies the propagation of action potential in cardiac tissue using the cable equation. Cable theory, one of the main problems of which is the calculation of the membrane potential and which has been developed in recent decades, is older than the cable equation itself. It is a variation of the equations developed by Lord Kelvin to model the propagation of electrical signals in underwater telegraphs. The cable theory was originally applied to conducting potentials in the axon, for example, by, [1]. Cardiomyocytes (heart muscle cells) differ from nerve axons in their shape and size - roughly they are very small cylinders. Variations of the cable equation led to passive one-dimensional (1D)

cable equations, which are monodomain and bidomain models and describe the electrical behavior of cardiac tissue cell membranes and propagation of action potentials.

Heart diseases are one of the leading causes of death in the world, and there are many scientific papers devoted to the study of the causes and mechanisms of heart problems. The study, [2], determined the distribution of intracellular, extracellular, and transmembrane potentials induced by current injection in the tissue in question. The study, [3], describes the simulation of excitation propagation in cardiac tissues based on nonlinear reaction-diffusion type models taking into account the monodomain model. The study, [4], investigates

the mathematical model of heart tissue based on the explicit representation of individual cells. A detailed mathematical model is used in, [5], to study the conductivity properties in small collections of cardiomyocytes.

Although the monodomain and bidomain models describe only the macroscopic behavior of syncytial (cellular) tissue, they are used to explain passive current measurement results in the lens, [6], measurements of cable constants, [7], and measurements of intracellular resistances in cardiac vessels in cardiac tissue filaments, [8], electrocardiogram, [9], [10], magnetocardiogram, [11], four-electrode impedance measurements, [12], and extracellular measurements of electrical potentials generated in atrial or ventricular muscles, [13], [14], [15], [16].

The current work discusses a one-dimensional model of continuously coupled myocytes. In this case, the electrical behavior in cardiac tissue is averaged for many cells. So, the distribution of the transmembrane potential in a single cell is studied. Using a monodomain model, the propagation of the transmembrane potential in a thin cylindrical excitable myocyte is studied in the absence of current at the beginning and end of the myocyte. A 1D mathematical model of the conductivity of discretely coupled myocytes is also discussed. Electrical behavior in the tissue is considered in individual myocytes, each of which is modeled as a continuum bound through conditions at cell boundaries that represent gap junctions. A stationary passive problem with Dirichlet boundary conditions is posed and solved analytically using the bidomain model. These problems are solved by the method of separation of variables. Numerical results of transmembrane potential propagation in cardiomyocytes are obtained using MATLAB software, and transmembrane isopotential contours, and 2D and 3D graphs of the obtained numerical results are presented.

2 Theoretical Aspects

The heart consists of transversely striated muscle tissue, which ensures the rapid spread of the wave of fiber contraction. As a result, all sections of the heart contract as a single entity. The homogeneous representation of cardiac tissue involves a large number of identical myocytes, which can be thought of as two interconnected spaces - intracellular and extracellular. The cells are connected by gap junctions (Figure 1).

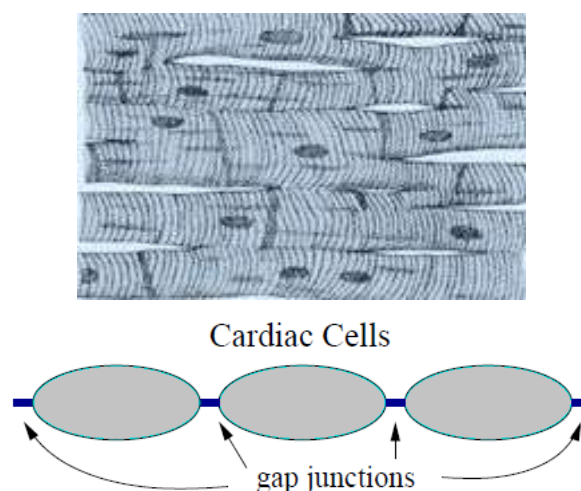


Fig. 1: Schematic drawing of cardiac tissue

The cardiac muscle action potential (membrane potential) is a brief change in voltage on the cell membrane in heart cells caused by the movement of charged atoms (ions) into and out of the cell via proteins called ion channels. The cell membrane separates extracellular and intracellular spaces with potentials φ_e and φ_i , while $V = \varphi_i - \varphi_e$ is the transmembrane potential.

An action potential is an excitation wave, which as a brief change of the membrane potential in the membrane of a living cell moves to a small area of an excited cell (neuron or cardiomyocyte), as a result of which the outer surface of this area becomes negatively charged compared to the inner surface of the membrane, while it is positively charged in a non-excitation state. Sometimes the action potential is called a propagating potential because the excitation wave is actively transmitted along the fiber of a neuron or muscle cell. Cardiomyocytes are approximately cylindrical (very small, measured in microns) whose length (e.g., x in the direction of the cylinder's long axis) is sufficiently greater than its diameter. So we can assume that the action potential of the cell depends only on the length variable, and the problem can be reduced to a single measurement. Thus, the article discusses both continuously and discretely coupled 1D myocyte models. Intracellular, extracellular, and transmembrane potentials are vector fields in space and time,

$$\text{i.e. } \varphi_i = \varphi_i(x, t), \varphi_e = \varphi_e(x, t), V = V(x, t).$$

The electrical behavior of the cell membrane of cardiac tissue and the propagation of the action potential are described by monodomain and bidomain models (equations). Both models use the representation of cardiac muscle as two interconnected spaces, intracellular and

extracellular. In contrast to the monodomain model, the bidomain model does not ignore the extracellular space; rather, it takes into account conductivity and the current flowing through it. The state of the bidomain system is described by intracellular φ_i and extracellular φ_e potentials. For these models, the search variable is the transmembrane potential $V = \varphi_i - \varphi_e$, and $V = \varphi_i$ for monodomain.

Using the passive 1D cable equation derived in Appendix A, the standard formulations for monodomain and bidomain models are presented below as extensions or variations of the cable equation.

2.1 Monodomain Model

The monodomain model (equation) for the transmembrane potential $V(x, t)$ is an extension of the cable equation presented in Appendix A. The equation relates the spatial distribution of the transmembrane potential to reaction conditions that locally control (determine) the transmembrane potential. 1D monodomain equation (A3) related to the kinetics of the time-dependent active ion channel $I_{ion}(t)$ and external stimulus $I_{stim}(t)$, can be written as:

$$\sigma_i \frac{\partial^2 V}{\partial x^2} = \chi \left(c_m \frac{\partial V}{\partial t} + I_{ion}(t) - I_{stim}(t) \right), \quad (1)$$

where $V(x, t)$ is the transmembrane potential, σ_i is the effective intracellular conductivity, χ is the tissue surface-to-volume ratio, and $c_m = 1 \mu F / cm^2$ is the membrane capacity. Let us divide equation (1) by χ and c_m and we will gain:

$$D \frac{\partial^2 V}{\partial x^2} = \frac{\partial V}{\partial t} + \frac{1}{c_m} (I_{ion}(t) - I_{stim}(t)),$$

where

$$D = \frac{\sigma_i}{\chi c_m}.$$

The monodomain equation is often presented in this form and D is described as a diffusion coefficient.

2.2 Bidomain Model

The bidomain model, [17], [18], is a phenomenological model that aims at encapsulating the action of single-cell ion channels in a homogenized representation of cardiac tissue consisting of a large number of identical myocytes. The model assumes the coexistence of two continuous domains (intracellular and extracellular)

at all points in space. A rigorous mathematical representation of the bidomain model was realized by, [19]. There are alternative mathematical formulations of the bidomain equations; the standard version presented here belongs to, [17].

The bidomain equations are derived from Maxwell's equations of electromagnetism with certain assumptions: 1) the first (quasi-static) assumption is that intracellular current can only flow between the intracellular and extracellular regions, and the intracellular and extra-myocardial regions can communicate with each other. So, the current flows into and out of extra-myocardial regions, but only in the extracellular area; 2) the second assumption is that the heart is isolated. So, the current leaving one domain must enter another. In addition, the current density in each intracellular and extracellular domain must be the same in magnitude but opposite in sign and can be determined as the product of the surface-to-volume ratio of the cell membrane and the transmembrane ionic current density per unit area.

According to Ohm's Law:

$$\mathbf{J} = \sigma \mathbf{E},$$

where \mathbf{J} is the electrical current, σ is the conductivity of space, and \mathbf{E} is the electric field.

Using the quasi-static assumption, the electric field \mathbf{E} is defined as the gradient of the scalar potential φ :

$$\mathbf{E} = -\nabla \varphi.$$

As a result, we will gain:

$$\mathbf{J} = -\sigma \nabla \varphi.$$

Assume, σ_i and σ_e are the conductivity of intracellular and extracellular spaces, respectively. According to Ohm's Law and the quasi-static assumption, we will gain the following expressions for \mathbf{J}_i (intracellular) and \mathbf{J}_e (extracellular) current densities in each domain:

$$\mathbf{J}_i = -\sigma_i \nabla \varphi_i.$$

$$\mathbf{J}_e = -\sigma_e \nabla \varphi_e.$$

The change in current density in each domain is equal to the current flowing through the membrane; under the second assumption, we will gain:

$$-\nabla \cdot \mathbf{J}_i = \nabla \cdot \mathbf{J}_e = A_m I_m,$$

where ∇ and $\nabla \cdot$ are the gradient and divergence operators, respectively, A_m is the ratio of the cell membrane surface to volume, and I_m is the transmembrane current density per unit area. By combining the two equations above, we gain

$$\nabla \cdot (\sigma_i \nabla \varphi_i) = A_m I_m, \quad (2)$$

$$\nabla \cdot (\sigma_e \nabla \phi_e) = -A_m I_m, \quad (3)$$

By summing up these equations, we will gain:

$$\nabla \cdot (\sigma_i \nabla \phi_i) = -\nabla \cdot (\sigma_e \nabla \phi_e).$$

Let us subtract $\nabla \cdot (\sigma_i \nabla \phi_e)$ from both sides. We will gain:

$$\nabla \cdot (\sigma_i \nabla \phi_i) - \nabla \cdot (\sigma_i \nabla \phi_e) = -\nabla \cdot (\sigma_e \nabla \phi_e) - \nabla \cdot (\sigma_i \nabla \phi_e).$$

By using denotation $V = \phi_i - \phi_e$ we will gain:

$$\nabla \cdot (\sigma_i \nabla V) = -\nabla \cdot ((\sigma_i + \sigma_e) \nabla \phi_e). \quad (4)$$

By inserting equation (2) in monodomain equation (1), we will gain:

$$\nabla \cdot (\sigma_i \nabla \phi_e) = \chi \left(c_m \frac{\partial V}{\partial t} + I_{ion} \right).$$

By subtracting and adding $\nabla \cdot (\sigma_i \nabla \phi_e)$ and considering $V = \phi_i - \phi_e$ notation, we will gain:

$$\nabla \cdot (\sigma_i \nabla V) = \chi \left(c_m \frac{\partial V}{\partial t} + I_{ion} \right). \quad (5)$$

By combining equations (4) and (5) and adding time- and space-dependent stimulus $I_s(x, t)$, a bidomain model is obtained:

$$\nabla \cdot (\sigma_i \nabla V) = -\nabla \cdot ((\sigma_i + \sigma_e) \nabla \phi_e) + I_{s1}, \quad (6)$$

$$\nabla \cdot (\sigma_i \nabla V) = \chi \left(c_m \frac{\partial V}{\partial t} + I_{ion} \right) - I_{s2},$$

where χ is the surface-to-volume ratio of the cell membrane, σ_i and σ_e are intracellular and extracellular conductivity, c_m is the membrane capacity per unit area, I_{ion} is the sum of all ionic currents, and I_{s_i} is the external stimulus.

It should be noted that the bidomain model can be reduced to a monodomain model in two particular cases: when the extracellular potential can be neglected because of the extracellular conductivity, and when the anisotropy ratio between the effective intracellular and extracellular conductivities is the same, [20]. In the latter case, the intracellular and extracellular conductivities are proportional and can be related as follows:

$$\sigma_e = \gamma \sigma_i$$

By inserting this expression in equation (6), we will gain:

$$\nabla \cdot \left(\frac{\gamma}{1+\gamma} \sigma_i \nabla V \right) = \chi \left(c_m \frac{\partial V}{\partial t} + I_{ion} \right) - I_{s2},$$

which is identical to the monodomain equation, if

we choose the effective conductivity $\sigma = \frac{\gamma}{1+\gamma} \sigma_i$.

3 Problem Statement and Solution

3.1 Monodomain Model

In this section, we discuss the 1D model of continuously coupled myocytes. Because of the assumption of continuity, in this case, the electrical behavior in the tissue is averaged over many cells. So, we will study the propagation of the transmembrane potential for one cell.

Consider a thin cylindrical excitable cell of length L . Let us solve the passive cable equation (see Appendix A) with the following boundary and initial conditions: 1) there is no current flowing into the cable (myocyte) (at the beginning of the cable) or out of the cable (at the end of the cable), and 2) at the beginning of time interval, the current is a function only of the spatial coordinate x of the cable. 1) is a problem analogous to the insulated-end beam thermal conductivity problem. Thus, the boundary and initial conditions will be written as follows:

$$\text{For } x = 0: V_{,x}(x, t) = 0, \quad (7)$$

$$\text{For } x = L: V_{,x}(x, t) = 0,$$

$$\text{For } t = 0: V(x, 0) = f(x). \quad (8)$$

Using the method of separation of variables (see Appendix B: after calculations of the integrals included in (B12) and elementary algebraic transformations) and considering the boundary (7) and initial (8) conditions, we will obtain the following expression:

$$\begin{aligned} V(x, t) &= \frac{2}{L} \frac{L^2}{2} + \frac{2}{L} \sum_{n=1}^{\infty} \left[\frac{L^2}{\pi n} \sin(\pi n) \right. \\ &\quad \left. + \left(\frac{L}{\pi n} \right)^2 (\cos \pi n - 1) \right] \cos \left(\frac{\pi n x}{L} \right) e^{(1 - (\lambda \pi n / L)^2) t / \tau_m} \\ &= L + 2L \sum_{n=1}^{\infty} \left(\frac{1}{\pi n} \sin(\pi n) + \frac{1}{(\pi n)^2} (\cos \pi n - 1) \right) \\ &\quad \times \cos \left(\frac{\pi n x}{L} \right) e^{(1 - (\lambda \pi n / L)^2) t / \tau_m}. \end{aligned}$$

3.2 Bidomain Model

The present section discusses the 1D mathematical model of conductivity in discretely coupled myocytes. Electrical behavior in the tissue is considered in individual myocytes, each of which is modeled as a continuum bound through conditions at the cell boundaries, which are gap junctions.

Consider a chain consisting of cylindrical myocytes of length L and radius a . The myocytes are connected through gap junctions, as described

by, [21]. The cylindrical coordinate system (r, θ, z) is defined by $x := z$ in the direction of the myocyte length. The extracellular space has a cross-sectional area $\Omega(x)$, which changes along x . The intracellular potential $V_i(x, t)$ is defined in myocytes, and extracellular potential $V_e(x, t)$ is defined in the extracellular space. The 1D bidomain model is constructed x by determining the average intracellular $V_i(x, t)$ and extracellular $V_e(x, t)$ potentials as well as the transmembrane potential $V_m(x, t) = V_i - V_e$.

The cable equation for each cell is as follows:

$$p \left(C_m \frac{\partial V_m}{\partial t} + I_{ion} \right) = \frac{\partial}{\partial x} \left(\frac{1}{r_i} \frac{\partial V_i}{\partial x} \right) = - \frac{\partial}{\partial x} \left(\frac{1}{r_e} \frac{\partial V_e}{\partial x} \right). \quad (9)$$

Here: $r_i = \frac{R_i}{A_i}$ and $r_e = \frac{R_e}{A_e}$, where R_i , R_e are resistances of intercellular and extracellular spaces, respectively. $A_i = \pi a^2$ and A_e are the average intracellular and extracellular cross-sectional areas of the cell, respectively, C_m the membrane capacity, and $p = 2\pi a$ the cell circumference. The intracellular current is given as $\frac{1}{r_i} \frac{\partial V_i}{\partial x}$ and is

continuous in the cell. I_{ion} is the sum of all ionic currents, which is taken as a constant current applied to all points of the cell membrane, i.e.:

$$I_{ion} = \frac{V_m}{R_m} = \frac{V_i - V_e}{R_m}.$$

Assuming that gap junctions behave as ohmic resistors, the potential drop at the junctions is proportional to the current flowing through the junctions.

$$\frac{[V_i]}{r_j} = \frac{1}{r_i} \frac{\partial V_i}{\partial x},$$

where $[V_i]$ is the leap in intracellular potential along the gap junction, and r_j is the effective resistance of the gap junction.

The steady-state passive problem with Dirichlet boundary conditions is solved by the method of separation of variables. For a constant stimulus at one end of the cable (Dirichlet boundary conditions), let us take the solution with a geometrically decaying solution, [21], $V_i(x+L) = \mu V_i(x)$, $V_e(x+L) = \mu V_e(x)$ for the decay constant $\mu < 1$. The decay constant is related

to the space constant λ_g by the following expression:

$$\mu = e^{-L/\lambda_g}.$$

For a given cell, the analytical solution of this stationary problem can be found, which for the n -th cell is proportional to:

$$\begin{pmatrix} V_i \\ V_e \end{pmatrix}_n = \mu^n \begin{pmatrix} \varphi_i \\ \varphi_e \end{pmatrix}.$$

Thus, in the case of the stationary state, equation (9) can be written as follows:

$$\frac{\partial}{\partial x} \left(\frac{1}{r_i + r_e} \frac{\partial \varphi_m}{\partial x} \right) - \frac{p \varphi_m}{R_m} = 0, \quad \varphi_m = \varphi_i - \varphi_e.$$

The solution of this equation is given as follows:

$$\varphi_m = c_{m1} \exp(kx) + c_{m2} \exp(-kx),$$

where $k^2 = \frac{p}{R_m} (r_i + r_e)$. So, the solutions are given

by the following formulas:

$$\varphi_i = \frac{r_i}{r_i + r_e} \varphi_m(x) + b, \quad \varphi_e = - \frac{r_e}{r_i + r_e} \varphi_m(x) + b,$$

Using the boundary conditions of current continuity and continuity of the extracellular potential and the leap in the intracellular potential at the gap junction, the constants are determined by the following formulas:

$$c_{m1} = \mu - e^{-kL}, \quad c_{m2} = \mu - e^{kL},$$

$$b = 2 \frac{r_e}{r_i + r_e} \frac{(\mu - e^{kL})(\mu - e^{-kL})}{\mu - 1},$$

where μ is the root of the following characteristic equation:

$$\frac{r_j k}{r_i + r_e} = \frac{R_j}{kL} = 2 \frac{(\mu - e^{-kL})(\mu - e^{kL})}{\mu(e^{kL} - e^{-kL})}.$$

$$R_j = \frac{L p r_j}{R_m} \quad \text{is the effective dimensionless}$$

resistance of the gap junction.

4 Numerical Realization

4.1 Realization of the Monodomain Model

The numerical simulations for the 1D model of continuously coupled myocytes in the absence of current at the beginning and end of the cable (cell), were performed using MATLAB software for the following data: time (τ ranges from 2.5 to 4.5 ms in humans) and length (λ ranges from 1.3 to 2.2 mm) for four pairs of constants:

- 1) $\tau = 2.5ms$, $\lambda = 1.3mm$;
- 2) $\tau = 2.8ms$, $\lambda = 1.6mm$;
- 3) $\tau = 3ms$, $\lambda = 1.8mm$ and
- 4) $\tau = 4.5ms$, $\lambda = 2.2mm$, myocyte (cell) length: $L = 135\mu m = 0.135mm$, spatial (lengthy) discretization $\Delta x = 6\mu m = 0.006mm$ and temporal discretization $\Delta t = 0.02ms$ were used. Numerical values of the transmembrane potential V were obtained during the variation of x (from $0.006mm$ to $0.135mm$) and t (from $0.02ms$ to $0.03ms$).

In practice, a system of contours (isolines) is often used to analyze the measurement results. For myocytes, some contours of transmembrane potential V for the plane area in the vector field of space (length) x and time t are presented. (It is possible to find such a system of points, in which numerical values of transmembrane potentials V are equal. By connecting them, we get lines of equal transmembrane potentials, so-called isopotential contours). Figure 2 shows myocyte transmembrane isopotential contours for four values of τ and λ . As Figure 2 shows, the transmembrane isopotential contours in all four cases look similar, in particular, all of them are almost elliptic lines, and only their numerical values differ slightly.

Figure 3 shows three-dimensional (3D) graphs of the distribution of the transmembrane potential V in the vector field of space and time for the myocyte for four values of τ and λ . As the Figure shows, in all cases, the 3D graphs look almost the same and only their numerical values differ slightly.

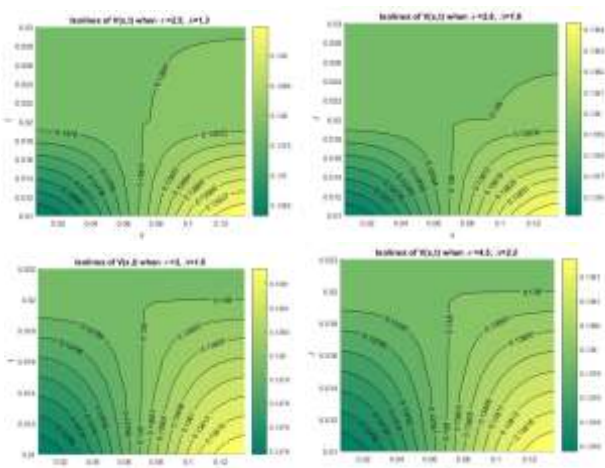


Fig. 2: Transmembrane isopotential contours for different fixed values of time and space constants (upper left figure: $\tau = 2.5ms$, $\lambda = 1.3mm$, upper right figure: $\tau = 2.8ms$, $\lambda = 1.6mm$, lower left

figure: $\tau = 3ms$, $\lambda = 1.8mm$, lower right figure: $\tau = 4.5ms$, $\lambda = 2.2mm$)

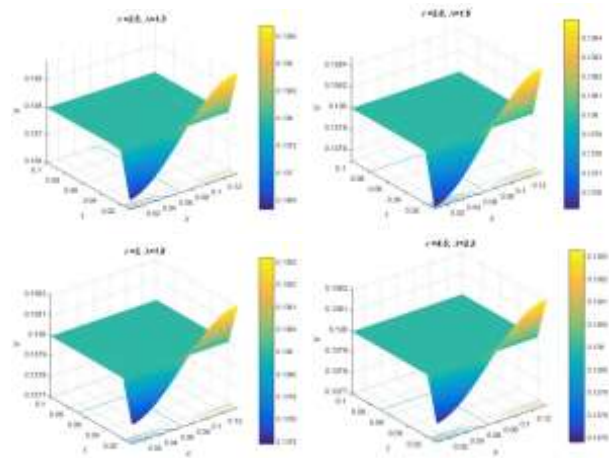


Fig. 3: 3D graphs of the distribution of V transmembrane potential in the $x t$ vector field for different fixed values of time and space constants (upper left figure: $\tau = 2.5ms$, $\lambda = 1.3mm$, upper right figure: $\tau = 2.8ms$, $\lambda = 1.6mm$, lower left figure: $\tau = 3ms$, $\lambda = 1.8mm$, lower right figure: $\tau = 4.5ms$, $\lambda = 2.2mm$).

Figure 4 gives the graphs of variation of V transmembrane potential along x for four different fixed constant values of τ any length λ and different fixed values of t , in particular: upper left figure: $t = 0.01ms$, upper right figure: $t = 0.02ms$, lower left figure: $t = 0.05ms$, lower right figure: $t = 0.09ms$. Figure 4 shows: 1) as the value of t increases different fixed constant values of τ and length λ , the graph of variation of transmembrane potentials get close to each other meaning that the transmembrane potential will change after some time only slightly when τ and λ change; 2) in all four cases, as $x \approx 0.075$, for all four values of time and length constants, the transmembrane potential $V(x,t) = 0.138$.

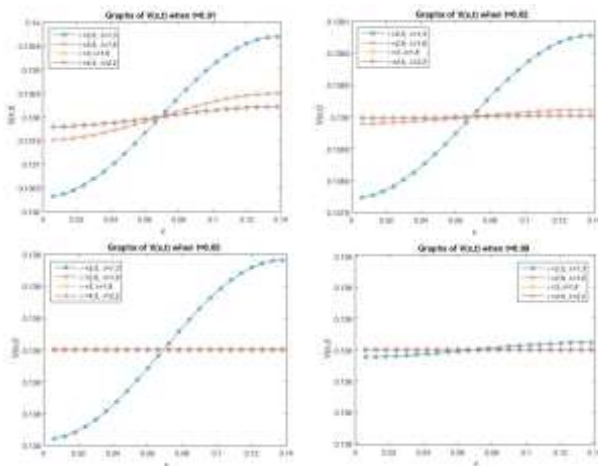


Fig. 4: Graphs of variation of transmembrane potential V along x for different fixed values of time τ and space λ constants and different fixed values of t , in particular: upper left figure: $t = 0.01ms$, upper right figure: $t = 0.02ms$, lower left figure: $t = 0.05ms$, lower right figure: $t = 0.09ms$.

Figure 5 shows the graphs of variation of transmembrane potential V as t changes for different fixed values of time τ and space λ constants and different fixed values of x in particular upper left figure: $x = 0.006mm$, upper right figure: $x = 0.012mm$, lower left figure: $x = 0.03mm$, lower right figure: $x = 0.054mm$. In all four cases, 2D graphs look very similar and only their numerical values differ slightly. Besides, in all four cases $t > 0.02$, transmembrane potential $V(x,t) = 0.138$.

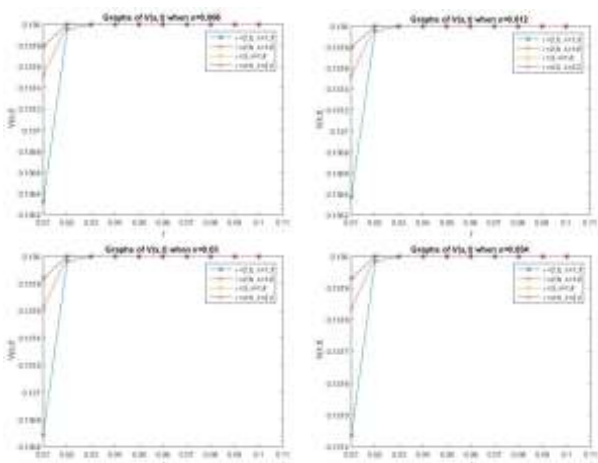


Fig. 5. Graphs of variation of transmembrane potential V , in case of t change, for different fixed values of time τ and space λ constants and different fixed values of x , in particular: upper left figure: $x = 0.006mm$, upper right figure:

$x = 0.012mm$, lower left figure: $x = 0.03mm$, lower right figure: $x = 0.054mm$.

4.2 Realization of the Bidomain Model

The 1D mathematical model of conductivity in discretely coupled myocytes discussed in section 3.2, was realized numerically, in particular, for 16 cells at fixed potentials at both ends of the myocyte in the steady state. Numerical simulation was done with MATLAB software for the following data based on the obtained analytical solution:

$$L = 0.012cm, \quad A_i = 4 \times 10^{-6} cm^2, \\ A_e = 1.5A_i = 6 \times 10^{-6} cm^2, \\ A_i = \pi a^2, a = \sqrt{4 \times 10^{-6} / \pi} \quad \lambda_g = 0.09cm,$$

$$R_m = 7000\Omega cm^2, \quad R_i = 150\Omega cm, \quad R_e = 75\Omega cm, \\ R_j = 110\Omega cm.$$

The graphs corresponding to the analytical solution are shown in Figure 6, in particular, graphs of changes in the intracellular potential V_i , extracellular potential V_e , and transmembrane potential V for different fixed values of space constant λ_g : upper left figure: $\lambda_g = 0.09mm$, upper right figure: $\lambda_g = 0.05mm$, lower left figure: $\lambda_g = 0.03mm$, lower right figure: $\lambda_g = 0.01mm$. As the figure shows, by reduction λ_g , the geometric decay of intracellular, intercellular, and extracellular transmembrane potentials accelerates.

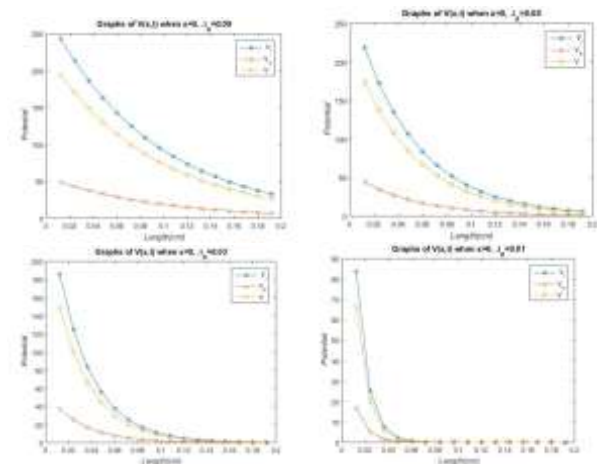


Fig. 6: Graphs of intercellular V_i , extracellular V_e , and transmembrane V potentials, as the functions of space for different fixed values of space constant (upper left figure: $\lambda_g = 0.09mm$, upper right

figure: $\lambda_g = 0.05mm$, lower left figure:
 $\lambda_g = 0.03mm$, lower right figure: $\lambda_g = 0.01mm$).

5 Conclusion

In this paper, the theoretical matters for models of cardiac electrophysiology are considered, including the introduction of single-cell action potential models and the continuum tissue model. Mathematically describing the local continuous or discontinuous excitation of tissue is the focus of this work.

The principal results presented in the paper can be formulated as follows:

- Using the passive 1D cable equation, the standard formulations for monodomain and bidomain models are given as extensions of the cable equation.
- The transmembrane potential propagation for a single cell is studied; in particular, the transmembrane potential propagation of a thin cylindrical excitable cardiomyocyte in the absence of current at the beginning and end of the cardiomyocyte is studied.
- A 1D mathematical model of the conductivity of discretely coupled cardiomyocytes is discussed. The electrical behavior in cardiac tissue is studied in individual cells, each of which is modeled as a continuum bound through conditions at cell boundaries that represent gap junctions.
- Using MATLAB software for the above problem, numerical results for the transmembrane potential are obtained, from which the contours of the transmembrane isopotential for the plane area in the vector field of length x and time t are construed. Some 2D and 3D graphs are plotted.
- One of the most surprising (interesting) results we obtained is that after a certain time, the transmembrane potential almost stops changing when τ and λ changes (Figure 4). It is important to verify these theoretical predictions experimentally.

Cardiovascular disease remains the leading cause of death worldwide, most notably, heart failure due to heart attack and fatal arrhythmias. The immediate cause of fatal cardiac arrhythmias is still not thoroughly understood, but in many cases, it may be related to an improper spread of the cardiac action potential. It should be noted that, despite many years of research, the distribution of the action

potential of the heart muscle is still not fully understood. So its study remains a pressing topic of many modern scientific studies.

This research can be used in electrophysiology to examine a wide range of arrhythmias to understand the etiology of the disease and figure out the solution. Also, the data can be used for some electrophysiologic medical devices to perform a comprehensive electrophysiologic study.

The work can be considered to be combined with artificial intelligence in the future for more efficacy of electrophysiologic diagnostic and treatment devices.

References:

- [1] Hodgkin AL, Rushton WAH. The electrical constants of a crustacean nerve fiber. *Proceedings of the Royal Society of London. Series B, Biological Sciences* 1946; 133: 444-479.
- [2] Sepulveda NG, Roth BJ, Wikswo JP. Current injection into a two-dimensional anisotropic bidomain. *Biophysical Journal* 1987; 55: 987-999.
- [3] Shuaiby SM, Hassan MA, et al. A finite Element Model for the Electrical Activity in Human Cardiac Tissues. *Journal of Ecology of Health & Environment* 2013; 1(1): 25-33.
- [4] Tveito A, Jæger KH, Kuchta M, Mardal K-A, Rognes ME. A Cell-Based Framework for Numerical Modeling of Electrical Conduction in Cardiac Tissue. *Frontiers in Physics* 2017; 5: Article 48.
- [5] Jæger KH, Edwards AG, McCulloch A, Tveito A. Properties of cardiac conduction in a cell-based computational model. *PLoS Computational Biology* 2019; 15(5): e1007042.
- [6] Eisenberg RS, Barcilon V, and Mathias RT. Electrical properties of spherical syncytia. *Biophysical Journal* 1979; 25:151-180.
- [7] Peskoff A. Electric potential in three-dimensional electrically syncytial tissues. *Bulletin of Mathematical Biology* 1979; 41(2): 163-181.
- [8] Roth BJ. *Longitudinal resistance in strands of cardiac muscle*. Ph.D. thesis, Vanderbilt University, Nashville, TN, 1987.
- [9] Tung L. *A bi-domain model for describing ischemic myocardial d-c potentials*. Ph.D. thesis. Massachusetts Institute of Technology, Cambridge, MA, 1978.
- [10] Miller WT, Geselowitz DB. Simulation studies of the electrocardiogram, 1. The normal heart. *Circulation Research* 1978; 43: 301-315.
- [11] Geselowitz DB, Miller WT. A bidomain model for anisotropic cardiac muscle. *Annals of Biomedical Engineering* 1983; 11: 191-206.
- [12] Plonsey R, Barr RC. The four-electrode resistivity technique is applied to cardiac muscle. *Ieee Transactions on Bio Medical Engineering* 1982; 29(7): 541-546.
- [13] Muller AL, Markin VS. Electrical properties of anisotropic nerve-muscle syncytia. 1. Distribution of the electric potential. *Biofizika* 1977; 22(2): 307-312.
- [14] Barr RC, Plonsey R. Propagation of excitation in idealized anisotropic two-dimensional tissue. *Biophysical Journal* 1984; 45: 1191-1202.
- [15] Plonsey R, Barr RC. Current flow patterns in two-dimensional anisotropic bi-syncytia with normal and extreme conductivities. *Biophysical Journal* 1984; 45:557-571.
- [16] Sepulveda NG, Wikswo JP Jr. Electric and magnetic fields from two-dimensional bi-syncytia. *Biophysical Journal* 1987; 51(4): 557-568.
- [17] Henriquez CS. Simulating the electrical behavior of cardiac tissue using the bidomain model. *Critical Reviews in Biomedical Engineering* 1993; 21(1):1-77.
- [18] Tung L. *A Bidomain Model for Describing Ischemic Myocardial D-C Potentials*. Ph.D. thesis, MIT, Boston, 1978.
- [19] Neu JC, Krassowska W. Homogenization of syncytial tissues. *Critical Reviews in Biomedical Engineering* 1993; 21(2):137-199.
- [20] Hunter P, Pullan A. Modeling total heart function. *Annual Review of Biomedical Engineering* 2003; 5: 147-177.
- [21] Keener J, Sneyd J. *Mathematical Physiology*, second edition. Springer, New York, NY, 2009.
- [22] Plonsey R, Barr RC. *Bioelectricity: a quantitative approach*. New York, NY, 2007.
- [23] Akar FG, Roth BJ, Rosenbaum DS. Optical measurement of cell-to-cell coupling in the intact heart using subthreshold electrical stimulation. *American Journal of Physiology-Heart and Circulatory Physiology* 2001; 281(2): H533-42.
- [24] Kamke E. *Handbook of Ordinary Differential Equations*. Moscow, Nauka, 1971.

APPENDICES

Appendix A. Derivating passive 1D cable equation

Let us consider a long enough thin cylindrical excitable cell. Let us denote the specific resistance of the cell by r_i , the membrane resistance by r_m , and the membrane capacity by c_m .

The variation of transmembrane potential V within a short interval Δx is formulated as follows: $V = -i_l r_i \Delta x$, where r_i is the resistance of the cell cytoplasm per unit length and i_l is the current along the membrane. Let us assume that $\Delta x \rightarrow 0$,

$$\frac{\partial V}{\partial x} = -i_l r_i. \quad (A1)$$

The current along the membrane can be described with the following formula: $\Delta i_l = -i_m \Delta x$, where i_m is the transmembrane current per unit of length. Again, letting $\Delta x \rightarrow 0$,

$$\frac{\partial i_l}{\partial x} = -i_m. \quad (A2)$$

Transmembrane current at every point x is the combination of capacitance current i_c and membrane leakage current corresponding to the membrane resistance i_r . The capacitance current within the membrane area of a given volume is expressed with the formula:

$$i_c = c_m \frac{\partial V}{\partial t}.$$

The current due to membrane resistance is expressed by Ohm's Law:

$$i_r = \frac{V}{r_m}.$$

By combining these two members, we gain:

$$i_m = c_m \frac{\partial V}{\partial t} + \frac{V}{r_m}.$$

Then, by inserting these two members in (A2) and by considering (A1) (from (A1), $i_l = -\frac{1}{r_i} \frac{\partial V}{\partial x}$), the

following expression is obtained:

$$\frac{\partial i_l}{\partial x} = \frac{\partial}{\partial x} \left(-\frac{1}{r_i} \frac{\partial V}{\partial x} \right) = -\frac{1}{r_i} \frac{\partial^2 V}{\partial x^2} = -\left(c_m \frac{\partial V}{\partial t} + \frac{V}{r_m} \right).$$

Therefore, the passive cable equation will be written down as follows:

$$\sigma_i \frac{\partial^2 V}{\partial x^2} = c_m \frac{\partial V}{\partial t} + \frac{V}{r_m}, \quad (A3)$$

where $\sigma_i = \frac{1}{r_i}$ denotes intercellular current.

Then, by an algebraic transformation of the passive cable equation, namely by multiplying equation (A3) by r_m , the number of parameters is reduced to two basic parameters. Thus, the passive cable equation will be written as follows:

$$\tau_m \frac{\partial V}{\partial t} = \lambda^2 \frac{\partial^2 V}{\partial x^2} - V, \quad (A4)$$

where λ is the constant of the space (length) of the passive cable equation and is expressed by the following formula:

$$\lambda = \sqrt{r_m \sigma_i} = \sqrt{\frac{r_m}{r_i}},$$

which determines the distance along the cell at which the injected potential decreases by factor e . By defining the spatial constant λ as the distance at which the potential at a cell point decreases by factor e , it can be calculated that for healthy tissue, the spatial constant is much greater than the length of an individual cell, in particular for normal cardiac excitation the spatial constant λ is much greater than the length of one myocyte ($\lambda = 1mm$, [22], or $\lambda = 1.5mm$, [23], compared to the average myocyte length of $0,1mm$). This means that the change in potential along the length of an individual cell is very small, and thus homogenizing the tissue to represent the continuum without considering the change in length of an individual cell is an acceptable approximation.

τ is a time constant and is defined by the following formula:

$$\tau = r_m c_m,$$

It determines the length of time over which the injected potential decreases by factor e . Space and time constants are useful parameters used to measure and characterize specific properties of excitable tissues.

Instead of passive membrane resistance, the currents, due to active ion channels, may be replaced by passive transmembrane currents. So:

$$i_r = \sum i_{ions},$$

where each ion i_{ions} is the transmembrane current due to the motion of a particular type of charge-

bearing ion. Then the equation of the passive cable can be written as follows:

$$\sigma_i \frac{\partial^2 V}{\partial x^2} = c_m \frac{\partial V}{\partial t} + \sum i_{ions}$$

Appendix B. Method of separation of variables

After separating the variables, let us write down $V(x, t)$ as follows:

$$V(x, t) = X(x)T(t) \tag{B1}$$

After substituting (B1) into equation (A4), we gain:

$$\tau_m XT' = \lambda^2 X''T - XT$$

Moving the members and equating them to the negative characteristic $(-k^2)$ yields:

$$\tau_m \frac{T'}{T} = \lambda^2 \frac{X''}{X} - 1 = -k^2$$

As a result, the following equations are gained:

$$\tau_m T' = -k^2 T, \tag{B2}$$

$$\lambda^2 X'' = (1 - k^2)X. \tag{B3}$$

The solution of equation (B2) is [24]:

$$T(t) = ce^{(-k^2 t / \tau_m)} \tag{B4}$$

As for the solution of (B3), if we assume that $k^2 > 1$, then the roots of the equation are complex. If $k^2 < 1$, then the roots will be real and the solution will be as follows, [24]:

$$X(x) = a \cosh x \sqrt{\frac{1 - k^2}{\lambda^2}} + b \sinh x \sqrt{\frac{1 - k^2}{\lambda^2}}$$

This will not serve because in this case, the boundary conditions do not allow for unique values of a and b , and only trivial solutions are obtained. So, if we consider that $k^2 > 1$, we will get the following expression, [24]:

$$X(x) = a \cos \left(\sqrt{\frac{1 - k^2}{\lambda^2}} x \right) + b \sin \left(\sqrt{\frac{1 - k^2}{\lambda^2}} x \right) \tag{B5}$$

By substituting equalities (B4) and (B5) into expression (B1), we will obtain:

$$V(x, t) = ce^{(-k^2 t / \tau_m)} \left[a \cos \left(\sqrt{\frac{1 - k^2}{\lambda^2}} x \right) + b \sin \left(\sqrt{\frac{1 - k^2}{\lambda^2}} x \right) \right] \tag{B6}$$

Boundary conditions $V_x(0, t) = 0$ and $V_x(L, t) = 0$ mean the following:

$$X'(0)T(t) = X'(L)T(t) = 0$$

Hence:

$$X'(0) = X'(L) = 0$$

The following expression is obtained from (B1), (B6) and $X'(0) = 0$:

$$X'(0) = -\sqrt{\frac{1 - k^2}{\lambda^2}} \left[a \sin \left(\sqrt{\frac{1 - k^2}{\lambda^2}} (0) \right) - b \cos \left(\sqrt{\frac{1 - k^2}{\lambda^2}} (0) \right) \right] = 0$$

The term containing sine drops out and $b = 0$ will remain. Thus, from (B5) we will gain:

$$X(x) = a \cos \left(\sqrt{\frac{1 - k^2}{\lambda^2}} x \right) \tag{B7}$$

By applying the second boundary condition $X'(L) = 0$, we will gain:

$$X'(L) = -\sqrt{\frac{1 - k^2}{\lambda^2}} \sin \left(\sqrt{\frac{1 - k^2}{\lambda^2}} (L) \right) = 0$$

Generally, $\sin(\alpha) = 0$, when $\alpha = \pi n$, $n = 1, 2, \dots$, thus, we will gain:

$$\sqrt{\frac{1 - k^2}{\lambda^2}} = \frac{\pi n}{L}, \quad n = 1, 2, \dots \tag{B8}$$

Hence:

$$k^2 = 1 - \left(\frac{\lambda \pi n}{L} \right)^2 \tag{B9}$$

By substituting equality (B8) into (B7), we will gain:

$$X(x) = a \cos \left(\frac{\pi n x}{L} \right), \quad n = 1, 2, \dots \tag{B10}$$

By substituting equalities (B9) and (B10) into (B6), we will gain:

$$V_n(x, t) = a \cos \left(\frac{\pi n x}{L} \right) c \cdot e^{[1 - (\lambda \pi n / L)^2] t / \tau_m}, \quad n = 1, 2, \dots$$

Now, let us insert $d_n = ac$

$$V_n(x, t) = d_n \cos \left(\frac{\pi n x}{L} \right) e^{[1 - (\lambda \pi n / L)^2] t / \tau_m}$$

Hence, we will have the Fourier decomposition with cosines:

$$V(x, t) = \frac{1}{2} d_0 + \sum_{n=1}^{\infty} d_n \cos \left(\frac{\pi n x}{L} \right) e^{[1 - (\lambda \pi n / L)^2] t / \tau_m} \tag{B11}$$

By considering the initial condition $V(x,0) = f(x)$, the exponential term drops out:

$$V(x,0) = \frac{1}{2}d_0 + \sum d_n \cos\left(\frac{\pi n x}{L}\right) = f(x).$$

The Fourier decomposition with cosines will be written down as follows:

$$d_n = \frac{2}{L} \int_0^L f(\xi) \cos\left(\frac{n\pi\xi}{L}\right) d\xi.$$

By substituting this into (B11), the following expression is obtained:

$$\begin{aligned} V(x,t) = & \frac{2}{L} \int_0^L f(\xi) d\xi \\ & + \frac{2}{L} \sum_{n=1}^{\infty} \int_0^L \left[f(\xi) \cos\left(\frac{\pi n \xi}{L}\right) d\xi \right] \\ & \times \cos\left(\frac{\pi n x}{L}\right) e^{-(\lambda \pi n / L)^2 t / \tau_m}. \end{aligned} \quad (B12)$$

Contribution of Individual Authors to the Creation of a Scientific Article (Ghostwriting Policy)

The authors equally contributed to the present research, at all stages from the formulation of the problem to the final findings and solution.

Sources of Funding for Research Presented in a Scientific Article or Scientific Article Itself

No funding was received for conducting this study.

Conflict of Interest

The authors have no conflicts of interest to declare.

Creative Commons Attribution License 4.0 (Attribution 4.0 International, CC BY 4.0)

This article is published under the terms of the Creative Commons Attribution License 4.0

https://creativecommons.org/licenses/by/4.0/deed.en_US